Arabian Journal of Chemistry (2016) 9, S829–S834

King Saud University

Arabian Journal of Chemistry

www.ksu.edu.sa
www.sciencedirect.com

ORIGINAL ARTICLE

Electrochemical synthesis and characterization of cubic magnetite nanoparticle in aqueous ferrous perchlorate medium

D. Gopi [a,b,*], M. Thameem Ansari [a], L. Kavitha [c,d]

[a] *Department of Chemistry, Periyar University, Salem 636 011, Tamilnadu, India*
[b] *Centre for Nanoscience and Nanotechnology, Periyar University, Salem 636 011, Tamilnadu, India*
[c] *Department of Physics, Periyar University, Salem 636 011, Tamilnadu, India*
[d] *The Abdus Salam International Centre for Theoretical Physics, Trieste, Italy*

Received 8 April 2011; accepted 20 August 2011
Available online 28 August 2011

KEYWORDS

Magnetization;
TEM;
SEM;
Oxidation;
Oxide materials;
Nanoparticle

Abstract Electrochemical synthesis of cubic magnetite nanoparticle (MNP) in ferrous perchlorate aqueous medium and its spectral investigations have been carried out. The structural property of MNP is evidenced by X-ray diffraction pattern shows the characteristic peaks. Further the vibrational frequencies of MNP are evaluated using FT-IR and Raman spectroscopic techniques. UV–visible spectroscopic studies show the possibility of surface plasmon resonance effect. The cubic structure of MNP has been confirmed by transmission electron microscope (TEM) technique and it is also evidenced by scanning electron microscope (SEM). The as-synthesized MNP shows superparamagnetic property which is confirmed by the vibrating sample magnetometer, hence it could be useful for synthesis of very ultra superparamagnetic iron oxide solution (VUSPIO) for cancer treatment.

1. Introduction

The synthesis of magnetite nanoparticle has been a field under intense investigation due to the novel properties and potentiality on the practical applications in the development of magnetic resonance imaging contrast agents, immunoassays and targeted drug delivery vehicles (Hao et al., 2010; Gupta and Gupta, 2005; Majewski and Thierry, 2007). The magnetic properties of magnetite nanoparticle have been exploited in a broad range of applications including magnetic seals and inks, magnetic recording media, catalysts, therapeutic agents for cancer treatment, high performance seals in space applications, eye surgery to repair damaged retina (Teja and Koh, 2009;

* Corresponding author at: Department of Chemistry, Periyar University, Salem 636 011, Tamilnadu, India. Tel.: +91 427 2345766; fax: +91 427 2345124.
E-mail address: dhanaraj_gopi@yahoo.com (D. Gopi).

Peer review under responsibility of King Saud University.

Production and hosting by Elsevier

http://dx.doi.org/10.1016/j.arabjc.2011.08.005

Massart, 1981; Massart and Cabuil, 1987; Bee et al., 1995). These applications demand the nanomaterials of specific sizes, shapes, surface characteristics and magnetic properties. The magnetite in nano size form exhibit superparamagnetic behavior at room temperature. In other words, they strongly magnetize under an applied magnetic field but retain no permanent magnetism once the field is removed (Bee et al., 1995; Boistelle and Astier, 1988). Thus, with these excellent properties, magnetite nanoparticles are suitable for bio medical applications such as cancer diagnosis (Cornell and Schwertmann, 2003; Dormer et al., 2005) and magnetically medicated separation of biomolecules (Cui et al., 2006). The traditional method for preparing magnetite nanoparticle is the chemical co-precipitation of Fe^{2+} and Fe^{3+} aqueous salt solutions in an alkaline medium. The MNPs synthesized by the conventional hydrothermal method (Daou et al., 2006) possess the high ratio of surface to volume and magnetization. Therefore, these MNPs are prone to aggregate and displaying increase in particle size. However, increasing the size of particles would surely add attraction to an external magnet and therefore limit their applications in the biomedicine (Teja and Holm, 2002; Wang et al., 2007; Xu and Teja, 2006; Hermanek et al., 2007). In this context, it is very hard to obtain the magnetite nanoparticles with diameter smaller than 25 nm with better magnetic properties because the difficulty in overcoming the problems of particle size, poly dispersity and the phenomenon of aggregation.

In this paper, we report the synthesis of MNPs through electrochemical route. The electrochemical synthesis of MNP has begun to emerge as an option among the conventional methods for the preparation of magnetic nanoparticle (Cabrera et al., 2008; Delatorre et al., 2009; Cao et al., 2006; Marques et al., 2008). Synthesis of MNP by electrochemical method have already been reported using organic amine compounds like tetra methyl ammonium chloride (Cabrera et al., 2008), triethanolamine (Delatorre et al., 2009), poly allyl amine hydrochloride (Cao et al., 2006) and with $Fe(NO_3)$ (Marques et al., 2008) either used as an electrolyte or as a surfactant with tedious electrode constructions. Envisaged by the above in mind, we report a facile method for the synthesis of MNP in an organic free especially amine free medium by electrochemical method using ferrous perchlorate aqueous solution with two electrode construction.

2. Materials and methods

2.1. Electrochemical synthesis of cubic magnetite nanoparticle

The metal iron sheets have been employed as anode and cathode, the dimension of electrodes were 1×1 cm^2 and 0.2 mm thickness to synthesize the nano-sized magnetite nanoparticles. The electrodes were pretreated by hydrochloric acid for 10–20 s to remove the unwanted layer on the surface of electrodes and finally washed with acetone and dried, prior to the electrochemical experiments. The iron (II) perchlorate is purchased from Alfa Aesar and used as received without further purification. The electrodes were immersed in 1 cm depth and placed directly opposite to each other. The electrochemical synthesis of magnetite nanoparticle is performed in homogeneous aqueous solution of $Fe(ClO_4)_2$, at the different concentrations of 0.01, 0.10 and 1.00 M of electrolyte (Table 1). The electrochemical reaction is carried out in galvanostat mode at various current densities of 40, 50 and 60 mA cm^{-2}, with constant stirring. The experiment is carried out with two reaction times of 1800 and 2700 s in every case and the reaction temperature was kept at 300 K. The MNP is deposited on cathode material and it is recovered carefully by scraping with glass rod and kept in poly tetra fluoro ethylene (PTFE) sample vial for further characterizations.

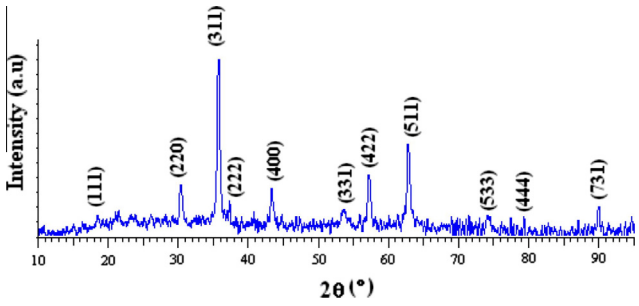

Figure 1 XRD pattern of MNP electrochemically synthesized from 0.1 M $Fe(ClO_4)_2$ at 50 mA cm^{-2}.

2.2. Characterization of magnetite nanoparticle

The phase composition and structure of the as-synthesized magnetite nanoparticle are determined by X-ray diffraction using a PANalytical model X'per PRO diffractometer with monochromatic Cu Kα radiation at the scanning speed of 0.5° (2θ) min^{-1}. The FT-IR spectrum of the magnetite nanoparticle is recorded from 400 to 4000 cm^{-1} region in Thermo Nicolet 5700 instrument using KBr pellet. Raman spectrum of MNP is obtained from Wi-Tec Raman spectrometer and sample was excited at 632.8 nm. The absorption spectrum of the magnetite nanoparticle is recorded using UV–visible spectrometer of CARY make by dispersing magnetite nanoparticle in water. The structural morphology of MNP is characterized by FEI TECNAI transmission electron microscope (TEM) at 200 keV by dispersing MNP in double distilled water and vig-

Table 1 Electrochemical reaction parameters.

Sample no.	Conc. of $Fe(ClO_4)_2$ (M)	Current density (mA cm^{-2})	pH	Reaction time (min)	Particle size (nm) measured by TEM
1	0.01	50	5.5	30	20 ± 2
2	0.1	50	5.8	30	15 ± 6
3	1.0	50	6.0	30	35 ± 9
4	0.1	40	5.8	45	18 ± 3
5	0.1	50	5.8	45	20 ± 5
6	0.1	60	5.8	45	18 ± 5

orously shaken before dropping the MNP on carbon coated copper TEM grids. Further the surface of MNP is elucidated by Philips make scanning electron microscope (SEM) at 20–30 keV electron beam radiation and the subsequent elemental analysis was performed using energy dispersive X-ray analysis (EDXA) system attached to the same instrument. The magnetic property of the sample is characterized by Lakeshore make vibrating sample magnetometer (VSM) with the applied magnetic field of ranging from −15,000 to 15,000 Gauss at room temperature 300 K.

3. Results and discussion

Electrochemical synthesis of magnetite nanoparticle was carried out in a 0.1 M solution of $Fe(ClO_4)_2$ at 50 mA cm^{-2} current density. The mean particle size was determined by TEM

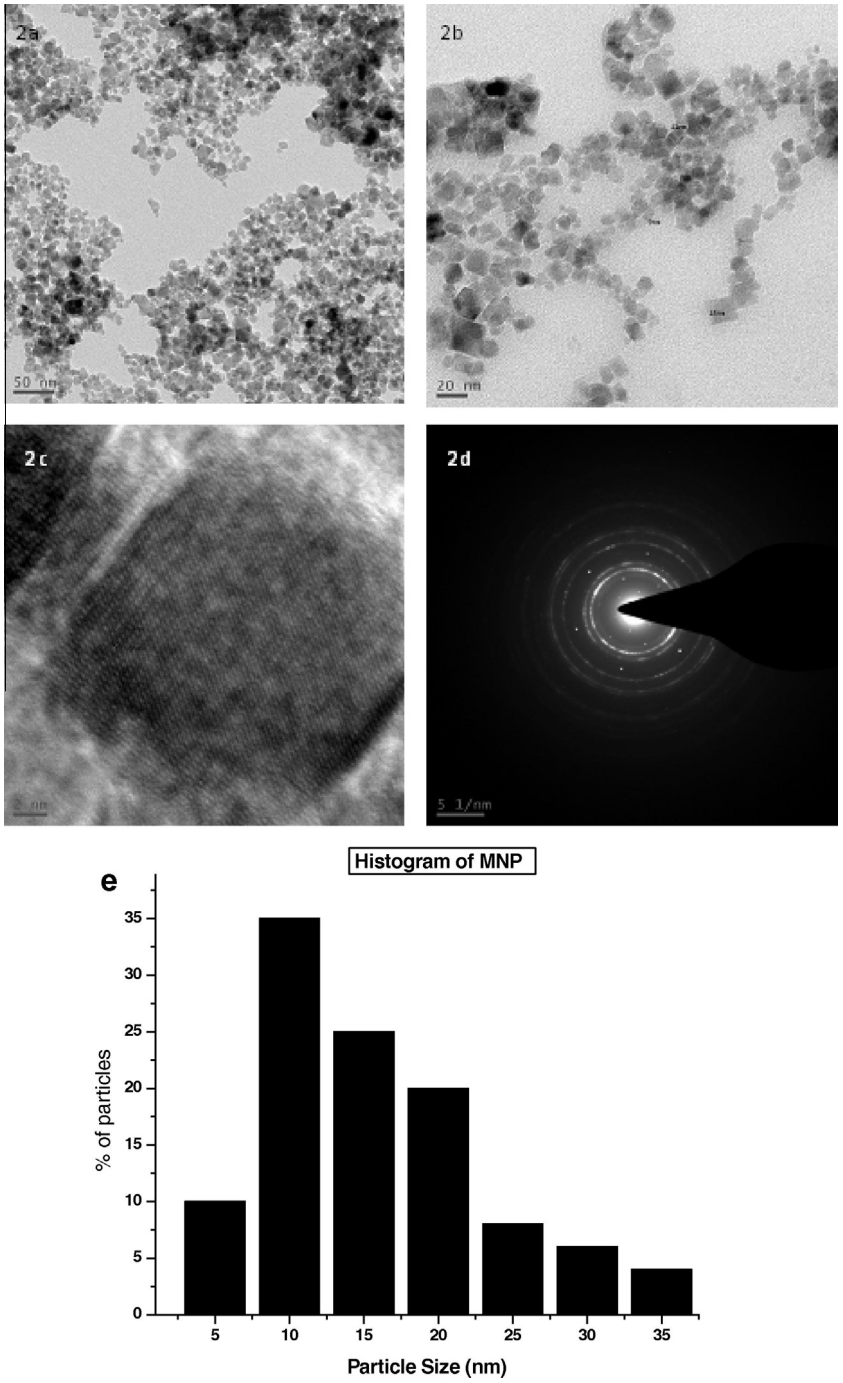

Figure 2 (a) TEM image of MNP electrochemically synthesized in 0.1 M $Fe(ClO_4)_2$ at 50 mA cm^{-2} (b) its high resolution images at 20 nm (c) at 2 nm and (d) its selected area electron diffraction pattern. (e) Histogram of the TEM image synthesized from 0.1 M $Fe(ClO_4)_2$ at 50 mA cm^{-2}.

analysis and is found to be 15 ± 6 nm. In order to analyze the effect of concentration of $Fe(ClO_4)_2$ on the particle size and size distribution of MNP, we have carried out a series of synthesis at various concentration ranging from 0.01 to 1 M.

Anodic reaction:

$$Fe \rightarrow Fe^{2+} + 2e^- \quad (1)$$

$$H_2O \rightarrow 2H^+ + 2e^- + 1/2O_2 \quad (2)$$

Cathodic reaction:

$$2H_2O + 2e^- \rightarrow H_2 + 2OH^- \quad (3)$$

$$2Fe^{2+} + Fe(ClO_4)_2 + 8H^+ + 4(1/2O_2) \rightarrow Fe_3O_{4(s)} + 2HClO_{4(l)} + 3H_{2(g)} \quad (4)$$

It is also found that the variation of current density does not influence much on the mean particle size of MNP. Thus when the current density is increased from 40 to 60 mA cm^{-2} for 0.1 M $Fe(ClO_4)_2$ the particle size was found to be around 20 ± 5 nm (Table 1). These results are in good agreement with the earlier results obtained on electrochemical synthesis of MNP by (Cabrera et al., 2008). It is also confirmed that the particle size distribution is inversely proportional to the current density to an increased diffusion rate of the generated MNPs with a decrement in Helmholz layer, where the reaction takes place.

It is already reported by Gnanaprakash et al. (2007) that the temperature and pH are playing major role in the synthesis of MNP by using conventional methods. Advantageously in our electrochemical reaction, the pH and temperature not necessarily be stabilized during the entire reaction course. However in order to control the agglomeration states between the particles, it is necessary to create an additional repulsive force to counterbalance the Van der Waals force. This can be achieved by the presence of a repulsive agent like perchloric acid ($HClO_4$) (Alboronoz and Jacobo, 2006). This is formed as a byproduct during electrochemical reaction course from the electrolyte. This perchloric acid can control the agglomerating tendency of the particles in colloidal solution. Further it is also observed that there is no significant change on the size and size distribution of MNP by increasing reaction period.

The powder X-ray diffraction pattern of magnetite nanoparticle synthesized from 0.1 M of $Fe(ClO_4)_2$ electrolyte at 50 mA/cm^{-2} is presented in Fig. 1. The characteristic peaks corresponding to the synthetic magnetite have been observed and the data is also referred with JCPDS card No. 89-2355. The following diffractions (2θ) were observed 18.29, 30.08, 35.43, 37, 43, 53, 56, 62, 73.9, 78.9 and 89.61 from corresponding hkl plane of 111, 220, 311, 222, 400, 331, 422, 511, 533, 444, and 731, respectively. Upon using the Scherrer's formula, the particle size of MNP corresponding to the most intense peak of 311 plane (2θ = 35.43) is found to be 15 nm which is also consistent with transmission electron micrographs.

$$D = 0.98\lambda/\beta\cos\theta, \quad (5)$$

where

$$\beta = X_{\text{diff}} \times \pi/180. \quad (6)$$

The as-synthesized MNPs is examined in transmission electron microscope (Fig. 2a–d) to confirm the structure and size of nanoparticle and its shows attractive cubic structured magnetite nanoparticle in monodispersed state. The high resolution transmission electron micrograph (Fig. 2c) and its selected area electron diffraction pattern (Fig. 2d) shows that the interatomic distance between atoms are 2.6 and 3 Å corresponds to the 311 and 220 plane of the as-synthesized magnetite nanocrystals respectively. These values are matched with powder X-ray diffraction pattern of the magnetite. The histogram (Fig. 2e) of the MNP depicts that 35% of the average size distribution is found to lien in the range of 10–15 nm and10% of the size distribution lies in the range of 2–5 nm.

The SEM image of electrochemically synthesized MNP from 0.1 M concentration of $Fe(ClO_4)_2$ as an electrolyte with applied current density of 50 mA cm^{-2} at a pH of 5.8, in time period of 30 min is depicted in Fig. 3a. From the SEM micrograph, it is evident that the cubic structured morphology and the nano sized magnetite particles were achieved by this method and the consecutive EDXA (Fig. 3b) measurement has also been done for this micrograph which detects the following elements Fe, Au, Si and O. Out of which gold and silica coming from the substrates and Fe and Oxygen coming from the samples.

Raman spectrum as depicted in Fig. 4 discriminates between the magnetite, maghemite and other iron oxide phases. The Raman modes of vibration of magnetite are unusually broad (typical) FWHMs around 40–50 cm^{-1}due to the presence of strong electro-phonon interaction in this compound (Chamritski and Burns, 2005; Shebanova and Lazor, 2003;

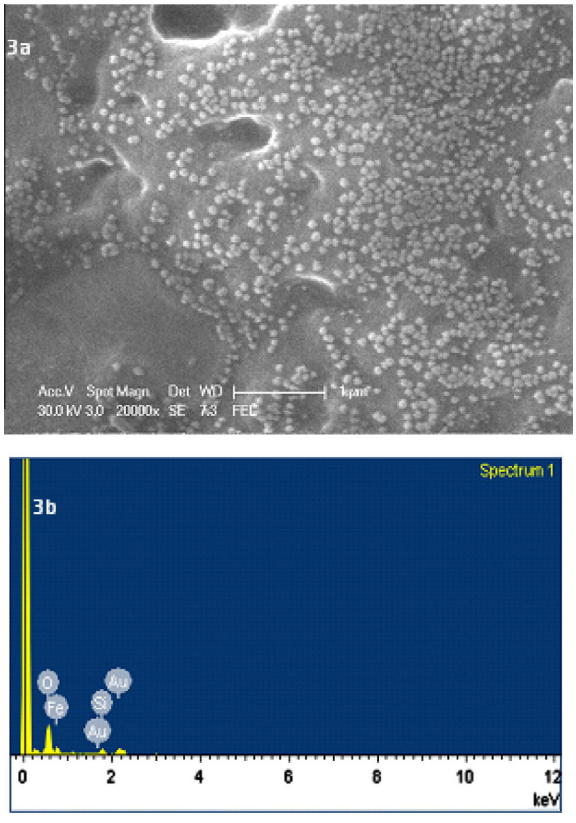

Figure 3 (a) SEM image of MNP electrochemically synthesized from 0.1 M $Fe(ClO_4)_2$ at 50 mA cm^{-2} and (b) its subsequent EDXA pattern.

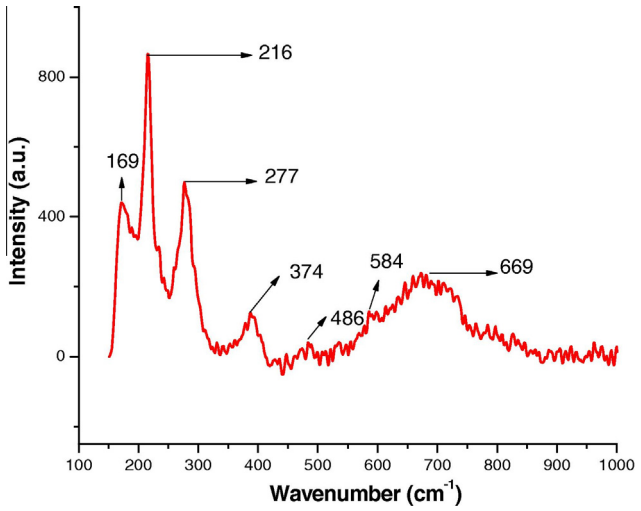

Figure 4 Raman spectrum of MNP carried out at laser power 18 mW excited at 632.8 nm.

Table 2 The Raman energy levels of MNP excited at 632.8 nm, A and B indicates position of Fe metal octahedral and tetrahedral geometry respectively.

Simulated value/cm^{-1} (Chamritski and Burns)	Experimental value/cm^{-1} (this work)	Ions involved	Symmetry species
241	216	A,O	$T_{2g}(1)$
296	277	O	$T_{2g}(2)$
505	486	B,O	E_{1g}
581	584	A,O	$T_{2g}(3)$
666	669	O	A_{1g}

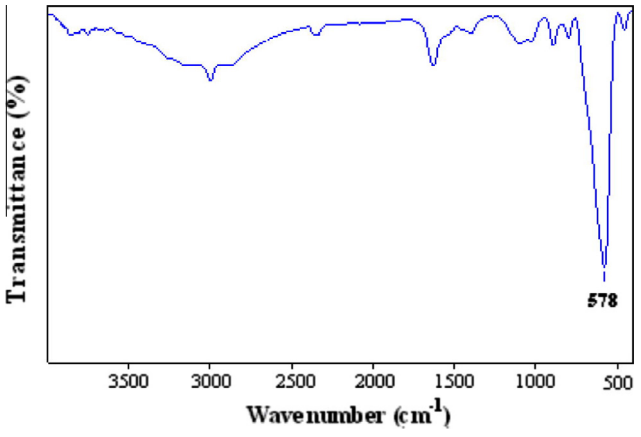

Figure 5 FT-IR spectrum of MNP electrochemically synthesized from 0.1 M of $Fe(ClO_4)_2$ at 50 mA cm^{-2}.

De Faria et al., 1997). Chamritski and Burns (2005) reported a computational study on the Raman active phonons of magnetite through atomistic simulation method and these values closely match with our Raman spectrum of MNP. The Raman shifts of theoretical and experimental values are tabulated (Table 2) with corresponding energy levels. The peaks at 216

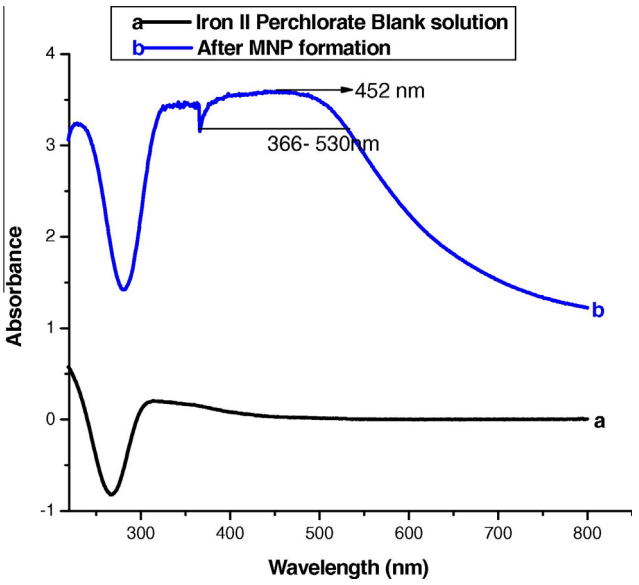

Figure 6 (a) UV absorption spectrum of initial electrolyte of 0.1 M of $Fe(ClO_4)_2$ and (b) colloidal solution of MNP.

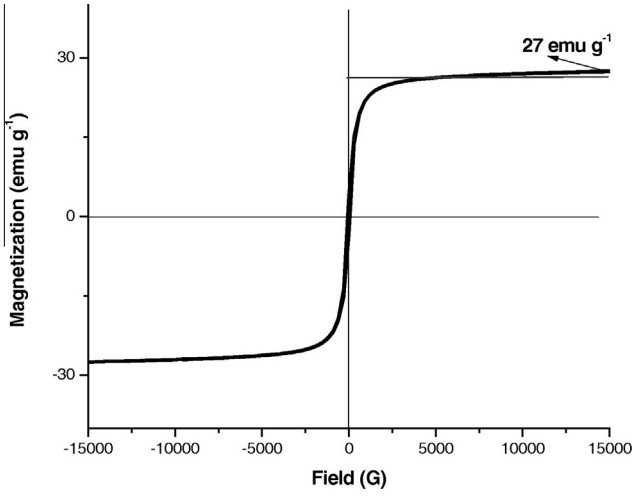

Figure 7 Hysteresis curve of as-synthesized MNP from 0.1 M of $Fe(ClO_4)_2$ at 50 mA cm^{-2}.

and 584 cm^{-1} were arising from $T_{2g}(1)$ and $T_{2g}(2)$ energy levels of metal–oxygen occupying octahedral positions respectively. The peak at 486 cm^{-1} from the E_{1g} energy level of metal–oxygen occupies at tetrahedral position. It indicates that the structure of obtained Fe_3O_4 nanoparticle is two Fe atoms are occupying at octahedral positions and one Fe atom is occupying the tetrahedral geometry which explaining the cubic structure of obtained Fe_3O_4 nanoparticles.

The strong peak at 578 cm^{-1} assigned in FT-IR spectrum (Fig. 5) indicates the presence of iron metal–oxygen stretching frequency. Probably the spectra around 550–650 cm^{-1} is assigned to M_T–O–M_O vibration, where M_T and M_O correspond to the metal occupying oxygen at the tetrahedral and octahedral positions, respectively. Further it evidences the presence of divalent tendency of electrochemically synthesized magnetite nanoparticles.

The UV absorption spectrum of blank ferrous perchlorate solution before the electrochemical reaction shows no characteristic peak (Fig. 6a) however after the electrochemical reaction the MNP colloidal solution shows a peak at 452 nm and further it exhibits a broad peak around 366–530 nm (Fig. 6b) which can be possible by the surface plasmon resonance effect in the magnetite nanoparticle. The optical part of the spectrum wavelength of the metal significantly changes when their size becomes less than the skin depth due to the collective electron oscillations in metal structures (Sarychev and Shalaev, 2000).

A typical vibrating sample magnetometer spectrum was also recorded for magnetite nanoparticle synthesized by electrochemical method at 0.1 M concentration of $Fe(ClO_4)_2$ at 50 mA cm^{-2}. The hysteresis curve (Fig. 7) demonstrates the superparamagnetic property of the magnetite nanoparticle at room temperature and it shows a very less coercive field (50 G). The applied magnetic field is in the range of −15,000 to 15,000 Gauss while the magnetization is not saturated in this applied magnetic field which is terminated at 27 emu g^{-1}.

4. Conclusion

The cubic magnetite nanoparticles have been successfully synthesized by electro-oxidation of iron in aqueous medium of ferrous perchlorate. This results in quite uniform particles with the mean size of 15 ± 6 nm which is evidenced from histogram of TEM image synthesized from 0.1 M of $Fe(ClO_4)_2$ at 50 mA cm^{-2}. The X-ray diffraction pattern and TEM images clearly support the presence of cubic magnetite nanoparticles. The FT-IR and Raman spectroscopic investigations confirm the characteristic vibrational frequency of MNP. Further UV spectrum shows the possibility of surface plasmon resonance effect in the metal oxide nano particles. This method is quite interesting since no micelles or stabilizing agent or surfactant was used to stop cluster growth, which occurs commonly in many conventional chemical routes. The MNP shows superparamagnetic property evidenced by vibrating sample magnetometer. Hence it could be used for synthesis of VUSPIO for cancer treatment.

Acknowledgements

One of the authors D.G. acknowledges the financial support from Indian Council of Medical Research (ICMR, IRIS ID No. 2010-08660, Ref. No: 5/20/11(Bio)/10-NCD-I), India, Department of Science Technology (DST), New Delhi, India and Tamilnadu State Council for Science and Technology (TNSCST) Tamilnadu in the form of major research projects. M.T. acknowledges the UGC-Networking Resource Centre of School of Chemistry, for PhD visiting student fellowship, Central Instruments Laboratory and Centre for Nanotechnology, University of Hyderabad, India for availing the instrumentation facilities. L.K. acknowledges the Junior Associateship from The Abdus Salam International Centre for Theoretical Physics (ICTP), Italy.

References

Alboronoz, C., Jacobo, S.E., 2006. J. Magn. Magn. Mater. 305, 12–15.
Bee, A., Massart, R., Neveu, S., 1995. J. Magn. Magn. Mater. 149, 6–9.
Boistelle, R., Astier, J.P., 1988. J. Cryst. Growth 90, 14–30.
Cabrera, L., Gutierrez, S., Menendez, N., Morales, M.P., Herraste, P., 2008. Electrochim. Acta 53, 3436–3441.
Cao, J., Zhitomirsky, I., Niewczaz, M., 2006. Mater. Chem. Phys. 96, 289–295.
Chamritski, I., Burns, G., 2005. J. Phys. Chem. B 109, 4965–4968.
Cornell, R.M., Schwertmann, U., 2003. The iron oxides: structure properties reactions. Occurrences and Uses. Wiley-VCH, Weinheim.
Cui, X.J., Antonietti, M., Yu, S.H., 2006. Small 2, 756–759.
Daou, T.J., Pourroy, G., Colin, S.B., Greneche, J.M., Bouillet, C.U., Legare, P., Bernhardt, P., Leuvrey, C., Rogez, G., 2006. Chem. Mater. 18, 4399–4404.
De Faria, D.L.A., Silva, S.V., De Oliveira, M.T., 1997. J. Raman Spectrosc. 28, 873–878.
Delatorre, R.G., Da Silva, R.C., Cruz, J.S., Garcia, N., Pasa, A.A., 2009. J. Solid State Electrochem. 13, 843–847.
Dormer, K., Seeney, C., Lewelling, K., Lian, G., Gibson, D., Johnson, M., 2005. Biomaterials 26, 2061–2072.
Gnanaprakash, G., Mahadevan, S., Jayakumar, T., Kalyanasundaram, P., Philip, J., Raj, B., 2007. Mater. Chem. Phys. 103, 168–175.
Gupta, A.K., Gupta, M., 2005. Biomaterials 26, 3995–4021.
Hao, R., Xing, R., Xu, Z., Hou, Y., Gao, S., Sun, S., 2010. Adv. Mater. 22, 2729–2742.
Hermanek, M., Zboril, R., Medrik, N., Pechousek, J., Gregor, C., 2007. J. Am. Chem. Soc. 129, 10929–10936.
Marques, R.F.C., Garcia, C., Lecante, P., Ribeiro, S.J.L., Noe, L., Silva, N.J.C., Amaral, V.S., Millan, A., Verelst, M., 2008. J. Magn. Magn. Mater. 320, 2311–2315.
Majewski, P., Thierry, B., 2007. Crit. Rev. Solid State Mater. Sci. 32, 203–215.
Massart, R., 1981. IEEE Trans. Magn. Mater. 17, 1247–1248.
Massart, R., Cabuil, V., 1987. J. Chem. Phys. 84, 967–973.
Sarychev, A.K., Shalaev, V.M., 2000. Phys. Rep. 335, 275–371.
Shebanova, O.N., Lazor, P., 2003. J. Raman Spectrosc. 34, 845–852.
Teja, A.S., Holm, L.J., 2002. The sun. In: Sun, Y.P. (Ed.), Supercritical Fluid Technology in Materials Science and Engineering, Synthesis, Properties, and Applications. Elsevier.
Teja, A.S., Koh, P.Y., 2009. Prog. Cryst. Growth Charact. Mater. 55, 22–45.
Wang, S.B., Min, Y.L., Yu, S.H., 2007. J. Phys. Chem. C 111, 355–3554.
Xu, C., Teja, A.S., 2006. J. Sup. Crit. Fluids 39, 135–141.